

8-15-2017

# Metastasis-Associated Protein 1 Deficiency Results in Compromised Pulmonary Alveolar Capillary Angiogenesis in Mice.

Jun-Hui Qin

Zhen-Yu Ke

Qiang Zhou

Li Wang

Yuan Liang

*See next page for additional authors*

Follow this and additional works at: [https://hsrc.himmelfarb.gwu.edu/smhs\\_biochem\\_facpubs](https://hsrc.himmelfarb.gwu.edu/smhs_biochem_facpubs)

 Part of the [Molecular Biology Commons](#)

## APA Citation

Qin, J., Ke, Z., Zhou, Q., Wang, L., Liang, Y., Wang, Y., Yang, T., Gao, X., Ye, J., Kumar, R., & Wang, R. (2017). Metastasis-Associated Protein 1 Deficiency Results in Compromised Pulmonary Alveolar Capillary Angiogenesis in Mice.. *Medical Science Monitor : International Medical Journal of Experimental and Clinical Research*, 23 (). <http://dx.doi.org/10.12659/MSM.905992>

This Journal Article is brought to you for free and open access by the Biochemistry and Molecular Medicine at Health Sciences Research Commons. It has been accepted for inclusion in Biochemistry and Molecular Medicine Faculty Publications by an authorized administrator of Health Sciences Research Commons. For more information, please contact [hsrc@gwu.edu](mailto:hsrc@gwu.edu).

---

**Authors**

Jun-Hui Qin, Zhen-Yu Ke, Qiang Zhou, Li Wang, Yuan Liang, Ying-Mei Wang, Tong Yang, Xing Gao, Jing Ye, Rekesh Kumar, and Rui-An Wang

Received: 2017.06.30  
Accepted: 2017.07.24  
Published: 2017.08.15

# Metastasis-Associated Protein 1 Deficiency Results in Compromised Pulmonary Alveolar Capillary Angiogenesis in Mice

Authors' Contribution:  
Study Design A  
Data Collection B  
Statistical Analysis C  
Data Interpretation D  
Manuscript Preparation E  
Literature Search F  
Funds Collection G

BCDE 1 **Jun-Hui Qin**  
C 1 **Zhen-Yu Ke**  
C 2 **Qiang Zhou**  
B 1 **Li Wang**  
B 1 **Yuan Liang**  
F 1 **Ying-Mei Wang**  
B 1 **Tong Yang**  
F 1 **Xing Gao**  
A 1 **Jing Ye\***  
C 3,4 **Rakesh Kumar**  
G 1,5 **Rui-An Wang\***

1 Department of Pathology, Xijing Hospital, Fourth Military Medical University, Xi'an, Shaanxi, P.R. China  
2 Chang'an Animal Health Inspection Institute, Xi'an, Shaanxi, P.R. China  
3 Department of Biochemistry and Molecular Medicine, School of Medicine and Health Sciences, George Washington University, Washington, DC, U.S.A.  
4 Cancer Research Program, Rajiv Gandhi Centre for Biotechnology, Thiruvananthapuram, Kerala, India  
5 Department of Pathology, Shenzhen Hospital, Southern Medical University, Shenzhen, Guangdong, P.R. China

\* Rui-An Wang and Jing Ye contributed equally to this work

**Corresponding Authors:** Rui-An Wang, e-mail: wangra@fmmu.edu.cn; Jing Ye, e-mail: yejing@fmmu.edu.cn

**Source of support:** This study was supported by the National Natural Science Foundation of China (NSFC): 30870923; 30971535

**Background:** The aim of this study was to investigate the effects of metastasis-associated protein 1 (MTA1) deficiency during angiogenesis of pulmonary alveolar capillaries in mice and to determine the molecular mechanisms involved.

**Material/Methods:** The expressions of MTA1, CD34, vascular endothelial growth factor (VEGF), alpha smooth muscle actin ( $\alpha$ -SMA), and HIF-1 $\alpha$  were analyzed in the lungs of *MTA1*-knockout (KO) and wild-type mice at embryonic day 18.5 and 2 months by quantitative PCR, immunoblotting, and immunohistochemistry. The morphological changes were investigated during pulmonary alveolar capillary formation. The heart weight/body weight (HW/BW) ratio and the size of the right ventricular wall cardiomyocytes were also measured. Regulation of MTA1 on HIF-1 $\alpha$  was determined *in vitro*.

**Results:** MTA1 deficiency reduced the number of pulmonary alveolar capillaries compared to the wild-type mice. *MTA1*-KO mice exhibited a decreased expression of HIF-1 $\alpha$  and VEGF in the lungs. The retarded growth of the *MTA1*-KO mice was also noticed during the first week after birth. Accordingly, MTA1 deficiency resulted in increased infant mortality. In surviving adult mice, MTA1 deficiency induced myocardial hypertrophy, highlighted by an increased heart weight/body weight ratio and larger cardiomyocytes. In cultured cells, HIF-1 $\alpha$  and VEGF levels were significantly upregulated upon MTA1 overexpression, suggesting a close relationship between all 3 molecules.

**Conclusions:** MTA1 participates in the formation of pulmonary capillaries via stabilization of HIF-1 $\alpha$ . This finding sheds new light on the function of MTA1 in lung development, opening new avenues for the diagnosis/treatment of related pulmonary diseases.

**MeSH Keywords:** **Mice, Knockout • Neovascularization, Physiologic • Persistent Fetal Circulation Syndrome**

**Full-text PDF:** <https://www.medscimonit.com/abstract/index/idArt/905992>

 2614  1  7  29



## Background

Metastasis-associated protein 1 (MTA1), a member of the nucleosome remodeling and decarboxylation complex (NuRD) family, has a profound role in pathological and physiological processes, and is highly expressed in mouse tissues and organs [1–3]. MTA1 regulates the expression of target genes due to its corepressor or coactivator activity [4]. In addition, MTA1 influences biological functions by modifying the stability of target proteins via deacetylation of non-histone proteins such as hypoxia-inducible factor 1- $\alpha$  (HIF-1 $\alpha$ ) by MTA1/histone deacetylases (HDACs) [5]. MTA1 expression correlates well with tumor angiogenesis, as well as with HIF-1 $\alpha$  and its target genes such as vascular endothelial growth factor (VEGF) [5–7]. Previous research has shown that specific HDACs induce angiogenesis and influence the stability of HIF-1 $\alpha$  in mice [8,9].

Vascular development in the lungs is a complex, multistep process controlled by several factors, including HIF-1 $\alpha$  and VEGF [10–12]. Notably, pulmonary vascular endothelial cells play a crucial role in regulating the pulmonary vascular system, and in maintaining barrier function and integrity of alveolar capillary membranes [13]. These cells, as well as other cell types in the lungs, express high levels of VEGF, which has been shown to be essential during fetal lung development, a process critically dependent on oxygen tension and angiogenesis [14]. Accordingly, administration of VEGF initiates the process of vessel formation [15,16]. Transcription of VEGF is regulated by HIF-1 $\alpha$ , a target of MTA1 [17,18]. In addition, increased HIF-1 $\alpha$  expression and its nuclear translocation are associated with pronounced angiogenesis [13,19]. These observations suggest that expression of HIF-1 $\alpha$  and VEGF is integral to the process of angiogenesis. Although HDACs induce angiogenesis and influence the levels of HIF-1 $\alpha$  in mice [8,9], the role of MTA1 and HIF-1 $\alpha$  in promoting angiogenesis during lung development remains unknown.

The present study was designed to determine the contribution of MTA1 and its downstream pathways during pulmonary vascular development in *MTA1*-knockout (KO) mice. Our results suggest that MTA1 facilitates the angiogenesis of pulmonary alveolar capillaries by stabilizing HIF-1 $\alpha$ , opening the possibility of new diagnosis and treatments for related pulmonary diseases.

## Material and Methods

### Animals and tissue collection

*MTA1*-KO mice were kindly provided by Dr. Rakesh Kumar's laboratory and were handled according to the Care and Use of Laboratory Animals guidelines of Fourth Military Medical

University. The animals were maintained under a 12-h light/12-h dark cycle with *ad libitum* access to water and chow diet. Before sacrificing and tissue collection, animals were fasted for 4 h. Tissues were collected and either directly fixed in 4% formaldehyde to produce paraffin sections or flash-frozen in liquid nitrogen followed by storage at  $-80^{\circ}\text{C}$  for further protein and mRNA analysis. The age of the fetus was determined relative to the date on which the vaginal plug was found, which was set to 0.5 E.

### Cell culture and transfection of an MTA1 overexpression vector

293T cells were grown in medium supplemented with 10% fetal bovine serum and 1 $\times$  antibiotic-antimycotic solution in a humidified incubator with 5% CO<sub>2</sub> at 37°C. Cell culture medium and additives were obtained from Gibco (Invitrogen). MLE-12 cells were obtained from the Cell Center of Fudan University (China). Cells were cultured in HITES (hydrocortisone, insulin, transferrin, estrogen) medium (Gibco) supplemented with 10% fetal bovine serum (FBS) and 2 mM glutamine at 37°C under conditions of 5% CO<sub>2</sub>. Transient transfections were performed using Lipofectamine 2000 (Invitrogen) according to the manufacturer's instructions.

### Antibodies and reagents

Sources of antibodies were as follows: MTA1 (D40D1) XP<sup>®</sup> rabbit mAb (#5647, Cell Signaling Technology); CD31 (PECAM-1) (D8V9E) XP<sup>®</sup> rabbit mAb (#77699, Cell Signaling Technology); rabbit anti-CD34 (BA0532, Boster Bio-Technology Co., LTD); rabbit anti-VEGF (BA0407, Boster Bio-Technology Co., LTD); ERG (A7L1G) Rabbit mAb (#97249, Cell Signaling Technology); rabbit anti-HIF-1 $\alpha$ /HIF1A (PBO245, Boster Bio-Technology Co., LTD); rabbit anti-alpha smooth muscle actin ( $\alpha$ -SMA) (ab5694, Abcam); and  $\beta$ -actin (Abcam). MTA1-piRES2-EGFP was from Dongao-Technology Co., LTD. Biotinylated rabbit anti-goat IgG secondary antibody (K0675, Dako), streptavidin-horseradish peroxidase (HRP) (K0675, Dako), and 3-3 diaminobenzidine (DAB) (Dako) enzyme-substrate complexes were used for immunohistochemical staining. HRP-conjugated rabbit anti-goat IgG (Sigma) was used for Western blot analysis.

### Heart weight/body weight (HW/BW) ratio

At 8 weeks, mice were weighted and executed by cervical vertebrae luxation. The heart was taken out and washed with normal saline to remove excess connective tissues and vessels. Bibulous paper was used to absorb any residual saline on the samples before they were weighed and measured. A Vernier caliper was employed to measure cardiomyocyte size.

**Table 1.** Primers for real-time PCR.

Name	Direction	Sequences
<i>MTA1</i>	Forward	5'-AGGAGGAAGAGGAGGAGGAGAATAT-3'
	Reverse	5'-GGCACCAGATCACATAGTTGTG-3'
<i>ERG</i>	Forward	5'-GTGGGCGGTGAAAGAATATGG-3'
	Reverse	5'-CTTTGGACTGAGGGGTGAGG-3'
<i>CD34</i>	Forward	5'-GATAATTGCCATTCCCATGC-3'
	Reverse	5'-CAGACTCCACCCTTACTTGAC-3'
<i>HIF-1<math>\alpha</math></i>	Forward	5'-AACAGTGACAAAAGACCGTA-3'
	Reverse	5'-ATGACTCCTTTCTGCTCT-3'
<i>VEGF</i>	Forward	5'-GAGATGAGCTTCTACAGCACAACA-3'
	Reverse	5'-GGAACATTTACAGTCTGCGGATCT-3'
$\beta$ -actin	Forward	5'-CGTTGACATCCGTAAAGACCTC-3'
	Reverse	5'-ACAGAGTACTTGCCTCAGGAG-3'

### Real-time polymerase chain reaction

Total RNA was extracted with TRIzol reagent (Invitrogen) and reverse-transcribed to cDNA using the PrimeScript RT reagent Kit (Takara) according to the manufacturer's protocol. Primers were synthesized by Sangon Biotech (Shanghai, China). All primer sequences are provided in Table 1. Quantitative PCR was performed using a 7500 Real-time PCR System and Power SYBR MasterMix (Applied Biosystems) following the manufacturer's instructions. Relative mRNA expression was calculated using the  $2^{-\Delta\Delta Ct}$  method with the Ct values normalized to  $\beta$ -actin as internal control.

### Protein preparation and western blot analysis

Total protein was extracted from tissues using RIPA buffer containing phenylmethylsulfonyl fluoride. After protein separation on 10% SDS-polyacrylamide gels and transfer to nitrocellulose, membranes were blocked with 5% (m/v) non-fat milk in 0.05% Tween-20/phosphate-buffered saline (PBS-T). The membranes were then washed (3 $\times$ 10 min) with PBS-T and further incubated with primary antibodies against MTA1 (1: 1000), HIF-1 $\alpha$  (1: 200), VEGF (1: 200), CD34 (1: 200), ERG (1: 1000), AQP5 (1: 1000), SPB (1: 1000),  $\beta$ -catenin (1: 1000), or  $\beta$ -actin (1: 3000) for 1.5 h at 37°C. After additional washes, the membranes were treated with anti-goat IgG HRP-conjugated secondary antibody (1: 10,000) in 5% non-fat milk-PBS-T for 1 h and washed again as above. Finally, an enhanced chemiluminescence system (Amersham Pharmacia) was used to develop the blots. Exposure times ranged from 40 s to 15 min. Signal intensities were semi-quantified and values were normalized to those of loading controls. Relative expression is presented in arbitrary units.

### Immunohistochemistry

Paraffin sections (4  $\mu$ m) were placed on poly-L-lysine-coated glass slides and stained according to standard immunohistochemical procedures. Briefly, after deparaffinization and washing in PBS, the sections were covered with 3% hydrogen peroxide in PBS for 15 min at room temperature to block endogenous peroxidase activity. The sections were blocked with 5% bovine serum albumin and incubated with primary antibodies against MTA1 (1: 50), HIF-1 $\alpha$  (1: 100), VEGF (1: 200),  $\alpha$ -SMA (1: 100), ERG (1: 200) or CD34 (1: 200) in a humidified chamber at 4°C overnight. After washing, the sections were incubated with biotinylated goat anti-rabbit IgG (Boster Biotechnology Co., LTD) for 1 h at 37°C. PBS (pH 7.2) was used to rehydrate the samples, followed by incubation with the avidin-biotinylated peroxidase complex for 45 min at 37°C. After washing in PBS, peroxidase activity was revealed using DAB according to the manufacturer's instructions.

### Red blood cell staining

After fixation, red blood cells were stained for hemoglobin using a pseudoperoxidase reaction with DAB. First, slides were placed in 0.05% DAB, 1% imidazole 1 M, and 0.1% H<sub>2</sub>O<sub>2</sub> in 50 mM Tris-HCl buffer (pH 7.4) for 10 min in a dark environment. They were then washed with demineralized water and counterstained using Harris hematoxylin for 2 min according to the manufacturer's instructions. Finally, the slides were rinsed with demineralized water and washed in running tap water to improve staining, dehydrated, cleared, and mounted.

### Transmission electron microscopy

Transmission electron microscopy was performed as follows: tissues were quickly removed and fixed with 2.5% glutaraldehyde, post-fixed in 1% osmium tetroxide in the same buffer for 1 h and dehydrated in acetone for embedding in Araldite. Semi-thin sections (thickness of 1  $\mu$ m) were stained with an alkaline solution of toluidine blue. Ultrathin sections were contrasted with lead citrate and uranyl acetate, and examined with an electron microscope.

### Statistical analysis

Data are presented as mean  $\pm$  standard error of the mean. Student's *t*-test and Mann-Whitney U test were used for parametric and nonparametric data, respectively. All statistical analyses were performed using GraphPad Prism V5.0 (GraphPad Software). Statistical significance was set at  $p < 0.05$ .

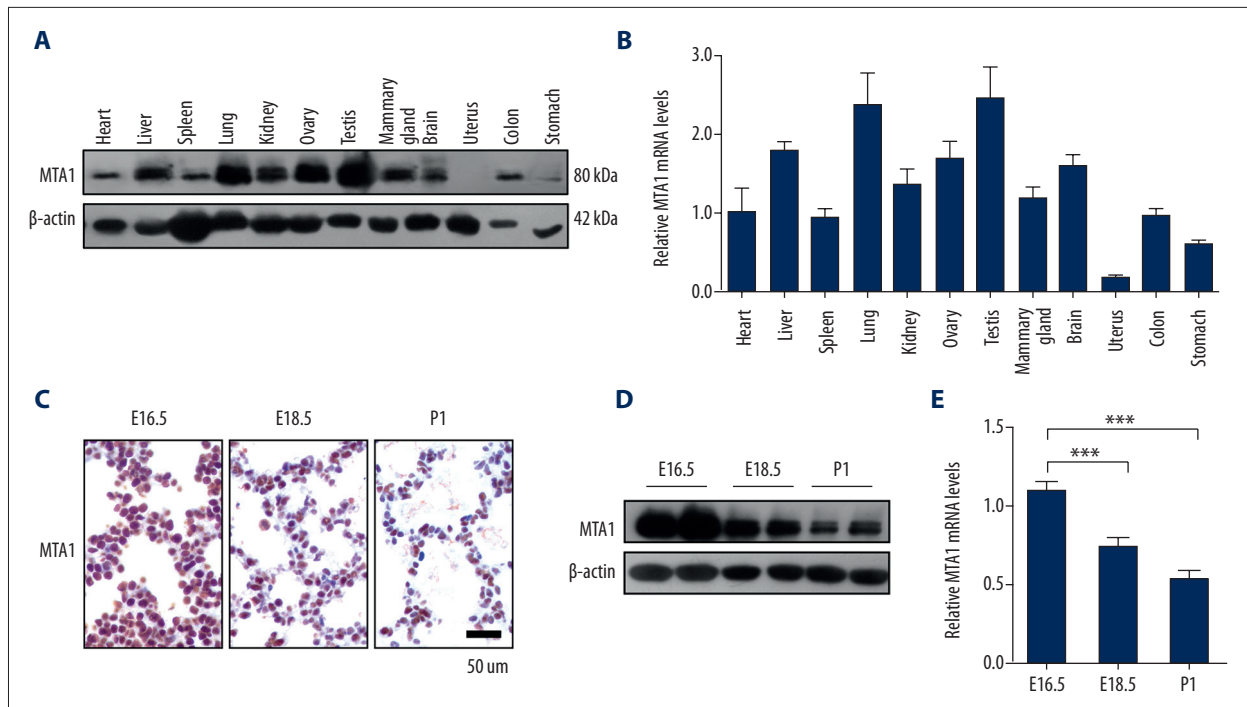


**Figure 1.** Expression of MTA1 in various tissues and organs of adult mice and during embryonic lung development. (A, B) MTA1 protein and mRNA expression by Western blotting and real-time PCR, respectively, in different tissues of adult wild-type mice. (C) immunohistochemical analysis demonstrates MTA1 expression in the lungs at E16.5, E18.5, and P1. (D) MTA1 protein expression in the lungs at E16.5, E18.5, and P1. Scale bar, 50  $\mu$ m. (E) A gradual, but significant decrease in the protein and mRNA levels of MTA1 was observed in the lungs from E16.5 to P1. Actin controls in A and D were blotted in parallel gels with the same amount of loading. n=6, \*  $P < 0.05$ , \*\*  $P < 0.01$ , \*\*\*  $P < 0.001$ .

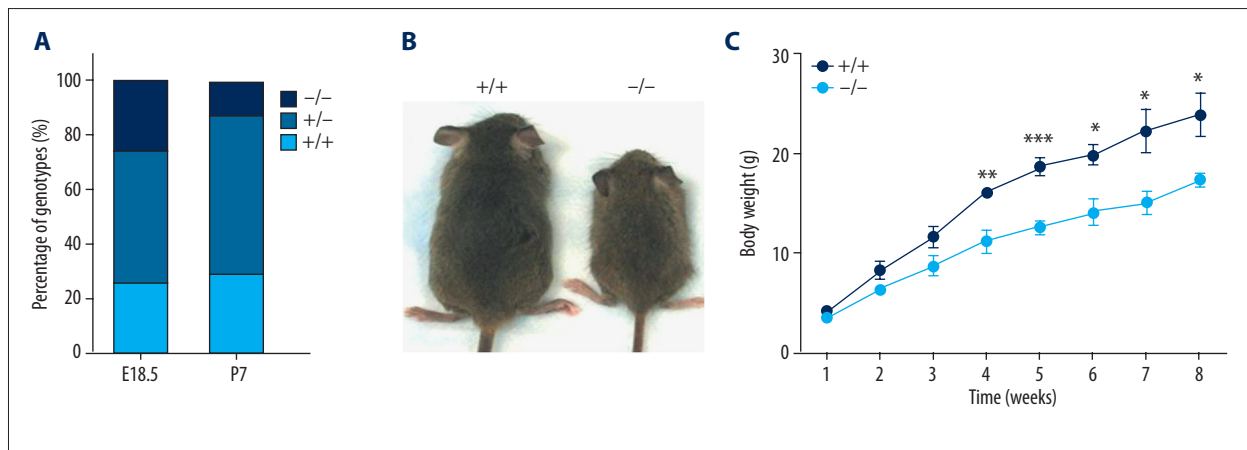


**Figure 2.** MTA1 deficiency increases infant mortality and impairs growth. (A) Postnatal mortality shows that over one-third of homozygous *MTA1*-KO mice died within 7 days after birth compared to wild-type mice. (B, C) MTA1-deficient mice that did survive exhibited retarded growth and markedly decreased body weight compared to wild-type mice. n=30, \*  $P < 0.05$ , \*\*  $P < 0.01$ , \*\*\*  $P < 0.001$ .

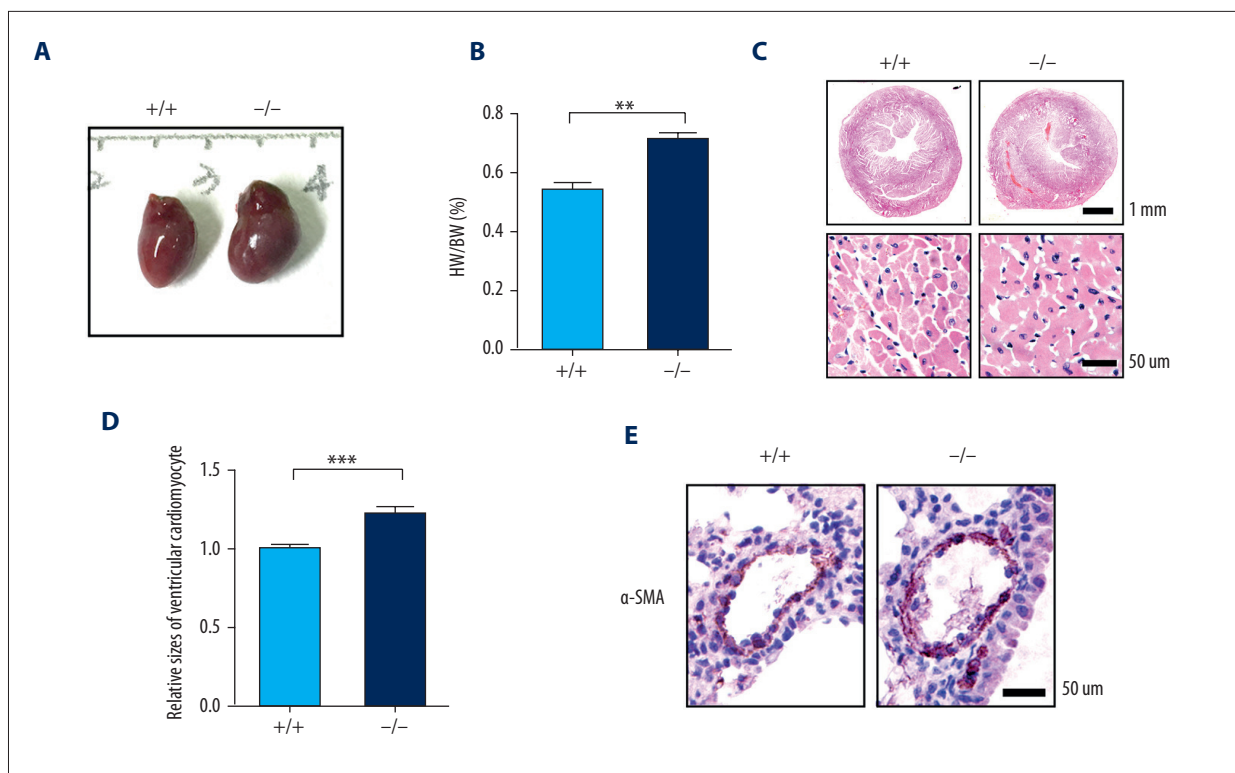


**Figure 3.** *MTA1*-KO mice present cardiac hypertrophy. (A) Representative images of HE-stained *MTA1*-KO and wild-type cardiac structures. Compared with wild-type animals, cardiomyocytes of *MTA1*-KO mice were bigger and hypertrophied ( $p < 0.05$ ). (B) The HW/BW ratio was significantly higher in *MTA1*-KO than in wild-type mice at 8 weeks of age ( $p < 0.05$ ), indicating *MTA1* deficiency induced myocardial hypertrophy in adult mice. (C, D) The size of right ventricular cardiomyocytes was significantly larger in *MTA1*-KO than in wild-type mice at 8 weeks of age ( $n = 10$ ), \*  $P < 0.05$ , \*\*  $P < 0.01$ , \*\*\*  $P < 0.001$ . (E)  $\alpha$ -SMA immunostaining highlights pulmonary artery wall thickening and hypertension in *MTA1*-KO mice ( $n = 6$ ). Scale bar, 50  $\mu$ m.

## Results

### MTA1 is abundantly expressed in mouse lung tissue

To determine the distribution of the MTA1 protein and its role in mice, we examined the levels of MTA1 in different tissues of mice by Western blot analysis. Our data indicate that MTA1 protein was present at high levels in the lungs, testis, and ovaries; at moderate levels in the brain, liver, mammary glands, and kidneys; at low levels in the heart, stomach, colon, and spleen; and could not be detected in the uterus (Figure 1A). The levels of MTA1 in various tissues corroborated well with MTA1 mRNA levels determined by real-time PCR (Figure 1B). An immunohistochemical analysis indicated that MTA1 was generally localized within cell nuclei (Figure 1C). We noticed a gradual decrease in the protein and mRNA levels of MTA1 expression during development from embryonic day 16.5 (E16.5) to postnatal day 1 (P1) in wild-type mice (Figure 1D, 1E). These findings suggest that MTA1 is expressed at high levels in the lung tissue, and the role of MTA1 in lung development was examined in subsequent studies.

### MTA1 deficiency increases infant mortality and retards growth

To investigate the function of MTA1 in mouse development, we evaluated mice at E18.5 and P7, which gave an estimate of postnatal mortality in the first week after birth. We found that, compared to wild-type mice, over one-third of homozygous *MTA1*-KO mice died within the first 7 days after birth (Figure 2A). However, some *MTA1*-KO mice did survive, exhibiting retarded growth and decreased body weight compared to wild-type littermates (Figure 2B, 2C). These observations suggest that MTA1 depletion increases infant mortality and inhibits growth.

### MTA1-deficient animals exhibit myocardial hypertrophy and pulmonary arterial hypertension

To further determine the role of MTA1 in the lungs, we investigated the effect of MTA1 deficiency on cardiac structure, because pulmonary capillary damage could cause pulmonary hypertension. The HW/BW ratio is an established parameter for evaluating cardiac structure. We report a significant increase

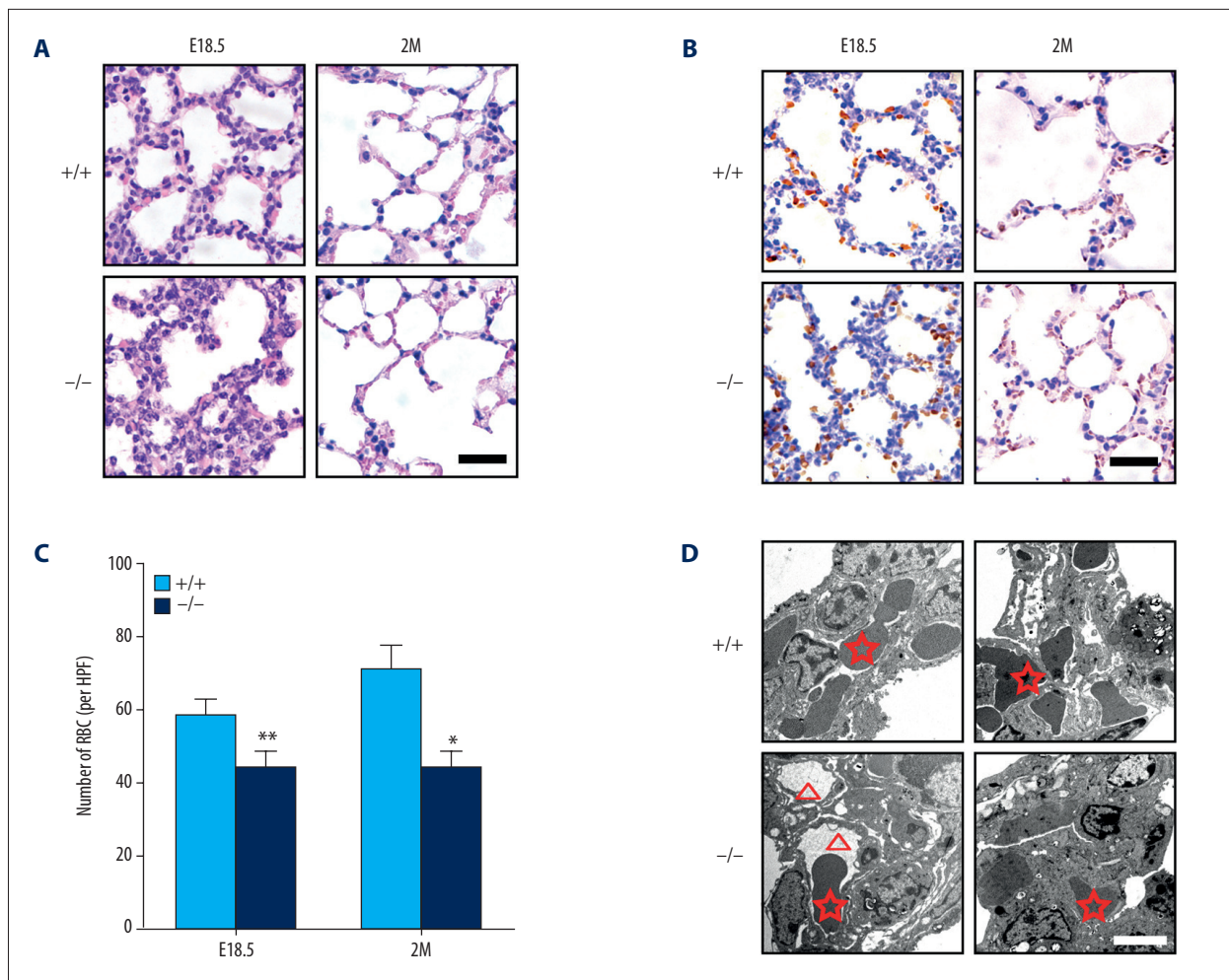


**Figure 4.** *MTA1*-KO mice display reduced vascularization of the lungs. (A–C) HE and Heme staining demonstrate a significantly reduced number of pulmonary capillaries and red blood cells in the lungs of *MTA1*-KO mice compared to wild-type animals.  $n=10$ , Scale bar, 50  $\mu\text{m}$ , \* $P<0.05$ , \*\* $P<0.01$ , \*\*\* $P<0.001$ . (D) Transmission electron micrograph showing a similar decrease in the number of pulmonary capillaries ( $\nabla$ ) and red blood cells (RBC,  $\star$ ) at E18.5 and 2M in *MTA1*-KO mice.  $n=6$ , Scale bar, 5  $\mu\text{m}$ .

in the HW/BW ratio in *MTA1*-KO compared to wild-type mice at 8 weeks of age ( $p<0.05$ ; Figure 3A, 3B). Accordingly, *MTA1* deficiency might induce myocardial hypertrophy in the adult mice due to a reduction of mature capillaries in pulmonary alveoli. To analyze the cardiac structure in further detail, we performed hematoxylin-eosin (HE) staining to calculate the thickness of the right ventricular wall. Consistent with an increase in the HW/BW ratio, cardiomyocytes' size was also significantly higher in *MTA1*-KO mice compared to wild-type mice (Figure 3C, 3D). The observation that *MTA1* deficiency induced pulmonary artery wall thickening and pulmonary arterial hypertension was further validated by  $\alpha$ -SMA immunostaining (Figure 3E). These results further indicate that *MTA1* deficiency leads to pulmonary hypertension and myocardial hypertrophy in adult mice.

#### **MTA1 deficiency impairs the formation of capillary beds**

To evaluate if capillary beds were affected in the lungs of *MTA1*-deficient mice, we used HE and Heme staining to assess the status of pulmonary capillaries and red blood cells (RBC). We noticed significantly fewer capillary beds and RBC in the lungs of *MTA1*-KO animals compared to wild-type littermates (Figure 4A–4C). This finding was confirmed at the E18.5 and 2M stage by transmission electron microscopy (Figure 4D). Immunohistochemistry results indicated that the expression level of CD34 was decreased in the lung tissue of *MTA1*-KO mice at E18.5 and 2M compared to the wild-type group (Figure 5A, 5B). However, the percentages of ERG positive cells were similar in the alveolar walls of wild-type and *MTA1*-KO mice at E18.5 and were increased significantly in the *MTA1*-deficient mice of 2M (Figure 5C). Accordingly, the same expression tendencies at both the protein and mRNA levels were confirmed at the

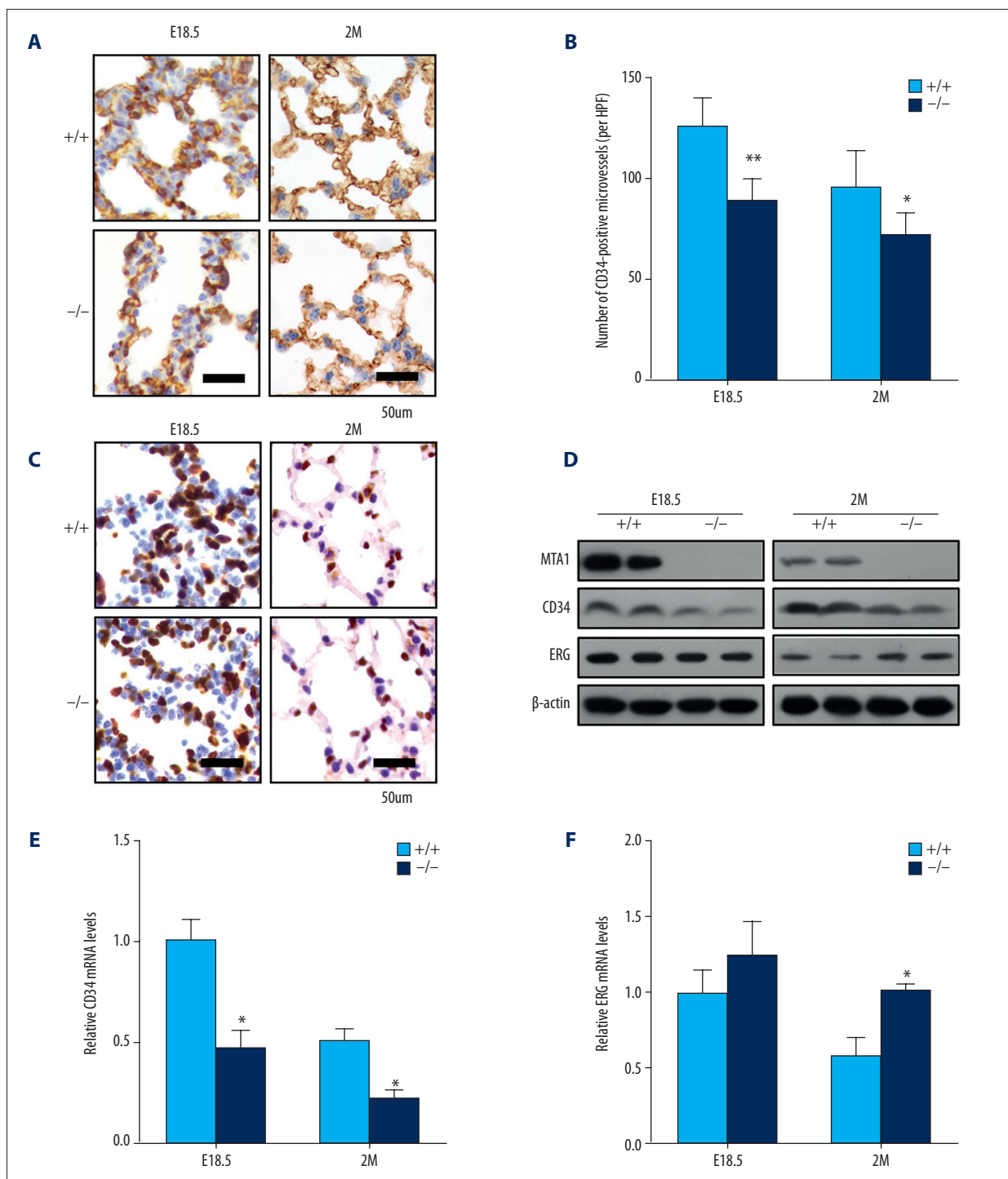


**Figure 5.** MTA1 deficiency impairs the formation of pulmonary capillary beds. (A, B) Immunohistochemistry results showed fewer CD34-positive cells in the lungs of MTA1-KO animals compared to wild-type mice at E18.5 and 2M. n=10, Scale bar, 50  $\mu$ m, \*  $P < 0.05$ , \*\*  $P < 0.01$ . (C) The percentages of ERG positive cells were similar in the alveolar walls of wild-type and MTA1-KO mice at E18.5 but were increased significantly in the MTA1-deficient mice of 2M. n=10, Scale bar, 50  $\mu$ m. (D) Western blot analysis highlights the downregulation of CD34 in the lungs of MTA1-KO mice at E18.5 and 2M compared to wild-type animals. ERG levels were similar at E18.5 but increased significantly in the MTA1-deficient mice of 2M. (E, F) The same expression tendencies of CD34 and ERG at mRNA levels were confirmed at the E18.5 and 2M stage by real-time PCR analysis. n=10, \*  $P < 0.05$ .

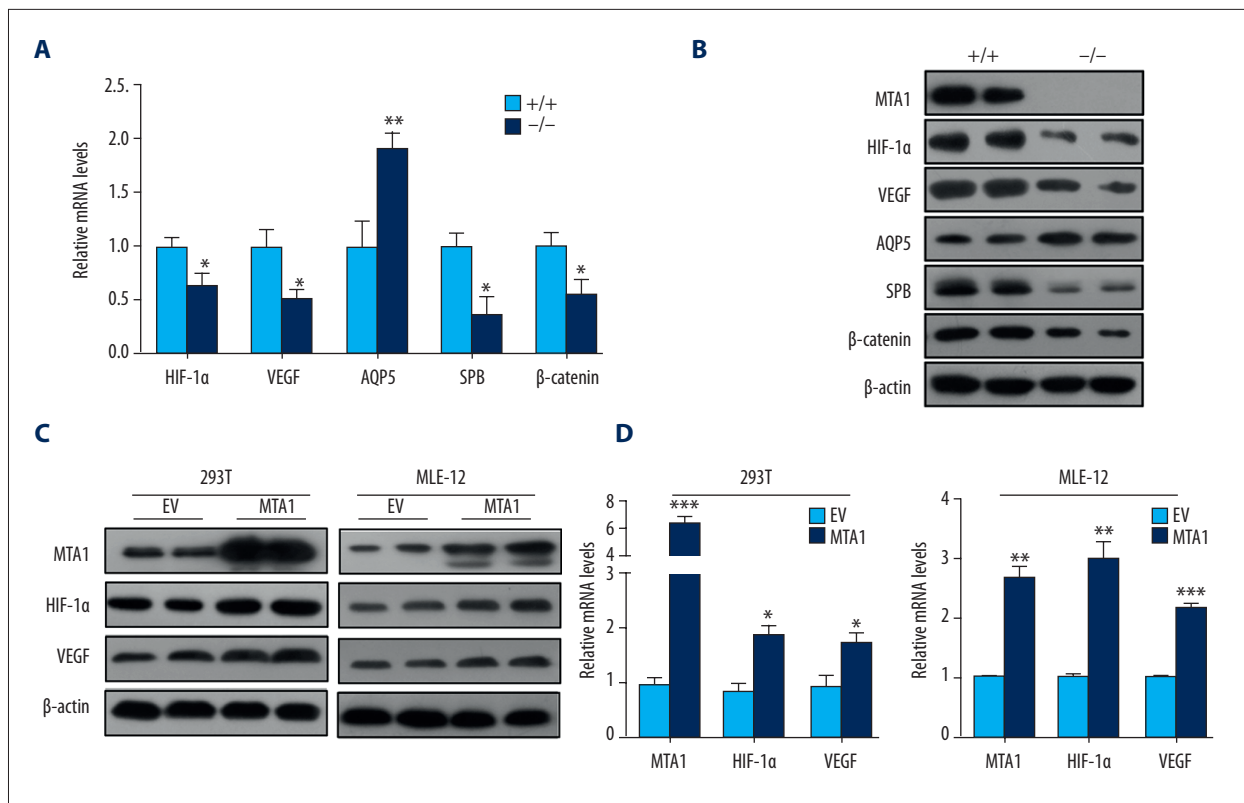


**Figure 6.** Regulation of HIF-1 $\alpha$  expression by MTA1. (A, B) Real-time PCR and Western blot analysis results indicated that MTA1 correlates well with many lung development-related factors such as VEGF, AQP5, SPB, and  $\beta$ -catenin. (C, D) Western blot and real-time PCR showed significant upregulation of HIF-1 $\alpha$  and VEGF in 293T and MLE-12 cells overexpressing MTA1 36 h after transfection. n=3, \*  $P<0.05$ , \*\*  $P<0.01$ , \*\*\*  $P<0.001$ .

E18.5 and 2M stage by Western blot and real-time PCR analysis (Figure 5D–5F). These results indicate that MTA1 deficiency could reduce the number of mature capillaries in pulmonary alveoli, suggesting MTA1 is involved in the development and maturation of pulmonary alveolar capillaries.

### MTA1 deficiency reduces HIF-1 $\alpha$ and VEGF levels in lung

MTA1 has been reported to modulate the stability of HIF-1 $\alpha$  through deacetylation by the MTA1/HDAC complex [6]. In addition to this, real-time PCR and Western blot analysis results indicated that MTA1 also correlates well with other lung development-related factors such as VEGF, AQP5, SPB, and  $\beta$ -catenin (Figure 6A, 6B). To investigate the regulatory role of MTA1 on the generation of pulmonary capillaries via HIF-1 $\alpha$  stabilization, we examined the effect of MTA1 on the status and gene expression of HIF-1 $\alpha$  and VEGF in cell models. As expected, MTA1 overexpression in both 293T and MLE-12 cells led to increased expression of HIF-1 $\alpha$  and VEGF compared to the control vector (Figure 6C), which was consistent with the increased HIF-1 $\alpha$  and VEGF mRNA levels (Figure 6D). These findings suggest that MTA1 expression stabilizes HIF-1 $\alpha$ , possibly via deacetylation. This, in turn upregulates the downstream expression of

VEGF and induces angiogenesis. However, this pathway was largely disrupted in the MTA1-KO mice, and results in the observed deficient formation of pulmonary capillaries.

### Discussion

MTA1 is a component of NuRD, which regulates gene expression as well as protein deacetylation in association with HDACs [20,21]. Previous studies have suggested that MTA1 enhances the stability of HIF-1 $\alpha$  by recruiting HDAC1 in cancer cells [5] and that MTA1 enhances the expression of VEGF by increasing the transcriptional activity of HIF-1 $\alpha$  [6]. In general, increased MTA1 expression in cancer has been shown to be closely associated with poor prognosis, increased tumor angiogenesis, and increased migration and metastasis [4,22–24].

However, cellular motility also plays a significant role in a variety of normal biological functions. For example, Li et al. have shown that MTA1 is abundantly expressed in the lungs of mice [2]. The underlying basis of the role of MTA1 in angiogenesis includes its upregulation under hypoxic conditions and stabilization of HIF-1 $\alpha$  by promoting its MTA1/HDAC1-dependent

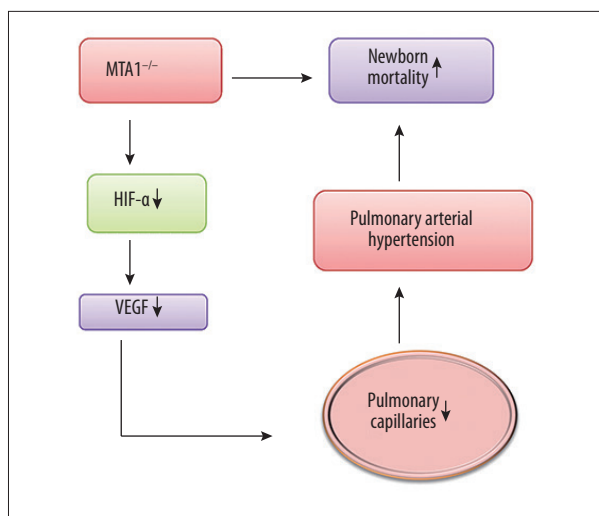


**Figure 7.** A correlation between the expression of MTA1 and HIF-1 $\alpha$  in the lungs. MTA1 is an active angiogenic regulator that deacetylates HIF-1 $\alpha$ . The MTA1- HIF-1 $\alpha$  axis feed into VEGF expression and the formation of pulmonary capillaries.

deacetylation on lysine 532 [5]. HIF1 is also fundamental to glycolysis, erythropoiesis, angiogenesis, and the prevention of apoptosis in response to low oxygen pressure, which enables cellular adaptation and survival in extreme conditions [25,26]. HIF-1 $\alpha$  activity appears to depend largely on the availability of HIF-1 $\alpha$  with a shorter half-life [5]. Regulation of HIF-1 $\alpha$  availability appears to occur predominantly at the post-translation level via protein stabilization. VEGF, one of the HIF-1 $\alpha$  primary targets, has been demonstrated to be involved in the pathogenesis of various lung diseases, such as bronchial pulmonary dysplasia, acute lung injury, emphysema, and pulmonary hypertension [13]. In this context, hypoxia is one of the strongest activators of VEGF expression [27–29]. Taken together, MTA1, HIF-1 $\alpha$ , and VEGF are all related to oxygen supply, making their expression and function potentially essential in

the lungs. However, regulation of HIF-1 $\alpha$  protein stability by MTA1 within the lungs was previously unknown.

To understand the effect of MTA1 deficiency on the formation of pulmonary alveolar capillaries and the expression of HIF-1 $\alpha$ , we investigated the functional consequences of MTA1 deficiency in the lungs of MTA1-KO mice. We observed that MTA1 was expressed at high levels in murine lung tissue and its depletion resulted in reduced VEGF and HIF-1 $\alpha$  levels, fewer pulmonary alveolar capillary beds, increased infant mortality, and retarded growth. These data suggest that MTA1 promotes the formation of pulmonary capillaries by deacetylating HIF-1 $\alpha$  and, subsequently, modulating HIF-1 $\alpha$  stability, increasing downstream VEGF expression, and inducing angiogenesis.

## Conclusions

In summary, this study identified a correlation between the expression of MTA1 and HIF-1 $\alpha$  in the lungs, in which MTA1 is an active angiogenic regulator responsible for deacetylating HIF-1 $\alpha$ . The MTA1/HIF-1 $\alpha$  axis then affects VEGF expression and the formation of pulmonary capillaries (Figure 7). These data enhance our understanding of MTA1 function during development and suggest that MTA1 may be a potential therapeutic target, providing new avenues for the diagnosis and treatment of related pulmonary diseases.

## Acknowledgements

We thank Professor Li Zhen (Department of Histology and Embryology, Fourth Military Medical University) for MTA1-pIRES2-EGFP vectors.

## Conflicts of interest

None.

## References:

- Simpson A, Uitto J, Rodecka U, Mahoney MG: Differential expression and subcellular distribution of the mouse metastasis-associated proteins Mta1 and Mta3. *Gene*, 2001; 273: 29–39
- Li W, Ma L, Zhao J et al: Expression profile of MTA1 in adult mouse tissues. *Tissue Cell*, 2009; 41: 390–99
- Kumar R, Wang RA: Structure, expression and functions of MTA genes. *Gene*, 2016; 582: 112–21
- Sen N, Gui B, Kumar R: Role of MTA1 in cancer progression and metastasis. *Cancer Metastasis Rev*, 2014; 33: 879–89
- Yoo Y, Kong G, Lee M: Metastasis-associated protein 1 enhances stability of hypoxia-inducible factor-1 $\alpha$  protein by recruiting histone deacetylase 1. *EMBO J*, 2006; 25: 1231–41
- Moon H, Cheon H, Chun KH et al: Metastasis-associated protein 1 enhances angiogenesis by stabilization of HIF-1. *Oncol Rep*, 2006; 16: 929–35
- Nagaraj S, Shilpa P, Rachaiah K, Salimath BP: Crosstalk between VEGF and MTA1 signaling pathways contribute to aggressiveness of breast carcinoma. *Mol Carcinog*, 2015; 54: 333–50
- Kim M, Kwon HJ, Lee YM et al: Histone deacetylases induce angiogenesis by negative regulation of tumor suppressor genes. *Nat Med*, 2001; 4: 437–43
- Bae M, Jeong JW, Kim SH et al: Tid-1 Interacts with the von Hippel-Lindau Protein and Modulates angiogenesis by destabilization of HIF-1 $\alpha$ . *Cancer Res*, 2005; 65: 2520–25
- Galambos C, deMello DE: Molecular mechanisms of pulmonary vascular development. *Pediatr Dev Pathol*, 2007; 10: 1–17
- Schittny JC: Development of the lung. *Cell Tissue Res*, 2017; 367: 427–44
- Qin W, Xie W, Xia N et al: Silencing of transient receptor potential channel 4 alleviates oxLDL-induced angiogenesis in human coronary artery endothelial cells by inhibition of VEGF and NF- $\kappa$ B. *Med Sci Monit*, 2016; 22: 930–36
- Lahm T, Crisostomo PR, Markel TA et al: The critical role of vascular endothelial growth factor in pulmonary vascular remodeling after lung injury. *Shock*, 2007; 28: 4–14

14. Vadivel A, Alphonse RS, Etches N et al: Hypoxia inducible factors promotes alveolar development and regeneration. *Am J Respir Cell Mol Biol*, 2013; 50: 96–105
15. Kanazawa H: Role of vascular endothelial growth factor in the pathogenesis of chronic obstructive pulmonary disease. *Med Sci Monit*, 2007; 13: RA189–95
16. Yamamoto Y, Baldwin HS, Prince LS: Endothelial differentiation by multipotent fetal mouse lung mesenchymal cells. *Stem Cells Dev*, 2012; 21: 1455–65
17. Voelkel N: Vascular endothelial growth factor in the lung. *Lung Cellular and Molecular Physiology*, 2005; 290: L209–21
18. Kim W, Safran M, Buckley MR et al: Failure to prolyl hydroxylate hypoxia-inducible factor alpha phenocopies VHL inactivation *in vivo*. *EMBO J*, 2006; 25: 4650–62
19. Sang H-y, Jin Y-l, Zhang W-q et al: Downregulation of microRNA-637 increases risk of hypoxia-induced pulmonary hypertension by modulating expression of cyclin dependent Kinase 6 (CDK6) in pulmonary smooth muscle cells. *Med Sci Monit*, 2016; 22: 4066–72
20. Sen N, Gui B, Kumar R: Physiological functions of MTA family of proteins. *Cancer Metastasis Rev*, 2014; 33: 869–77
21. Xue Y, Wong JM, Moreno GT et al: NURD, a novel complex with both ATP-dependent chromatin-remodeling and histone deacetylase activities. *Mol Cell*; 1998; 2: 851–61
22. Toh Y, Nicolson GL: Properties and clinical relevance of MTA1 protein in human cancer. *Cancer Metastasis Rev*, 2014; 33: 891–900
23. Mazumdar A, Wang RA, Mishra SK et al: Transcriptional repression of oestrogen receptor by metastasis-associated protein 1 corepressor. *Nat Cell Biol*, 2001; 3: 30–37
24. Jang K, Paik SS, Chung H et al: MTA1 overexpression correlates significantly with tumor grade and angiogenesis in human breast cancers. *Cancer Sci*, 2006; 97: 374–79
25. Greijer A, de Jong MC, Scheffer GL et al: Hypoxia-induced acidification causes mitoxantrone resistance not mediated by drug transporters in human breast cancer cells. *Cell Oncol*, 2005; 27: 43–49
26. Tai TC, Wong-Faull DC, Claycomb R, Wong DL: Hypoxic stress-induced changes in adrenergic function role of HIF1 alpha. *J Neurochem*, 2009; 109: 513–24
27. Tuder R, Voelke NF: Pulmonary hypertension and inflammation. *J Lab Clin Med*, 1998; 32: 16–24
28. Zhang G, Feng GY, Guo YL et al: Correlation between liver cancer pain and the HIF-1 and VEGF expression levels. *Oncol Lett*, 2016; 13: 77–80
29. Lee S, Goldfinger LE: RLIP76 regulates HIF-1 activity, VEGF expression and secretion in tumor cells, and secretome transactivation of endothelial cells. *FASEB J*, 2014; 28: 4158–68